Use of the Super Homogenization Method for Fast Reactor Analysis

Tung D. C. Nguyen[a], Tuan. Q. Tran[a], Kiho Kim[b], Deokjung Lee[a*]
[a]*Ulsan National Institute of Science and Technology (UNIST), 50 UNIST-gil, Ulsan 44919, Republic of Korea*
[b]*Korea Institute of Nuclear Safety, 62 Gwahak-ro, Yuseong-gu, Daejeon 34142, Republic of Korea*
[*]*Corresponding author: deokjung@unist.ac.kr*

1. Introduction

Recent studies have been successfully demonstrated the feasibility of employing the Monte Carlo (MC) code to generate multigroup cross-section (MG XS) generation for the nodal diffusion codes in the full-core analysis of liquid metal fast reactors (LMFRs). Nevertheless, applying only these MG XS in the diffusion codes would not guarantee a good consistency with the reference MC code solutions in the case of rodded cores. Therefore, this paper aims to evaluate the capability of the Super Homogenization (SPH) method that is particularly implemented to enhance the accuracy of the XSs in the control rod regions and their surroundings. In this work, the SPH method is briefly introduced and tested on a medium-size sodium fast reactor (SFR) core – MET-1000, specified in the OECD/NEA benchmark [1]. The XS data is prepared by the MC code MCS [2-3] and converted to a compatible database for the nodal diffusion code RAST-K [4] to simulate the full core problem. The diffusion results are obtained at the un-rodded and rodded state and verified against the reference full-core MCS solutions.

2. Computer Codes

Two UNIST in-house computer codes are used in this work: the MC code MCS and the nodal diffusion code RAST-K.

MCS is a 3D continuous-energy neutron-physics code for particle transport based on the MC method, under development at UNIST since 2013 [2]. MCS can conduct criticality runs for reactivity calculations and fixed source runs for shielding problems. MCS has been designed from scratch since 2013 to conduct whole-core criticality simulations with pin-wise depletion and thermal/hydraulic feedback. Recently, MCS has been featured with the XS generation capability [3].

The RAST-K (R2) code has been developed at UNIST for diffusion full-core calculations [4]. It adopts the 3D nodal method with MG coarse mesh finite difference acceleration technique to solve steady-state and transient problems with assembly-level nodes. Lately, the triangular polynomial expansion nodal method has been implemented in RAST-K for fast reactor analysis.

3. Benchmark Description

To evaluate the accuracy of the XSs generated by MCS and the feasibility of the SPH method, a modular metal-fueled 1000 MWth SFR (MET-1000) specified in the OECD/NEA benchmark [1] is selected for analysis, which its radial core layout is shown in Fig. 1. The MET-1000 core has 180 drivers, 114 radial reflectors, 66 radial shields, and 19 control subassemblies (SAs). It composes of two zones, the inner core zone and outer core zone, which contain 78 and 102 driver SAs, respectively. Each driver SA consists of 271 fuel pins arranged in a triangular pitch array with HT-9 cladding and is enclosed by a hexagonal HT-9 duct. Each fuel rod is divided into four axial zones: the lower reflector, fuel, bond sodium, and gas plenum (Fig. 2a). The radial pattern of the driver SA is illustrated in Fig. 2b. Two independent safety-grade reactivity control subsystems are employed: the primary and secondary control systems containing 15 and 4 control SAs, respectively.

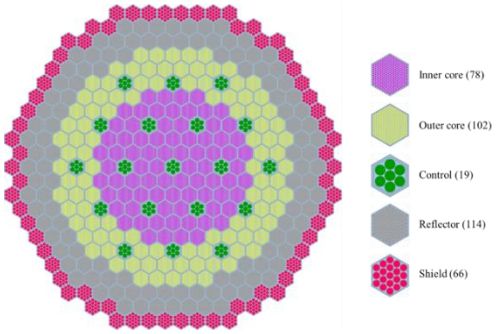

Fig. 1. MET-1000 radial core layout.

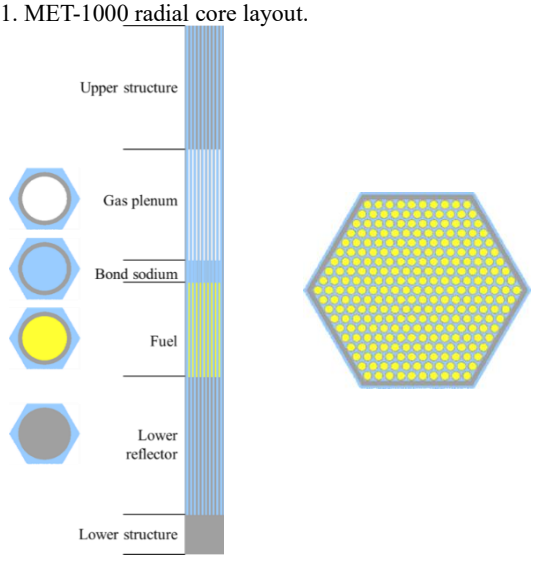

(a) (b)

Fig. 2. MET-1000 driver SA: (a) axial layout and (b) radial layout.

4. Solution of the MET-1000 Whole-core Problem

4.1 Generation of the MG XSs and Application of the SPH Method

A general approach to tallying the 24-group (as in Table 1) XSs of each component of the fast reactor is discussed. The target XSs for each type of fuel SA are obtained employing a single 2D model of a fuel SA with reflective boundary conditions. For the non-multiplying regions except radial reflector, all the homogenized XSs are sampled using 2D supercell models, as shown in Fig. 3. To approximate the flux in these regions in the core, they are located at the center of the model and surrounded by the fuel SAs. In the case of the reflector SAs, the radial reflector model, as illustrated in Fig. 4, is used for generating XS.

Table I: 24-group Energy Structure

No.	Upper E (MeV)	Lower E (MeV)
1	1.96403E+01	1.00000E+01
2	1.00000E+01	6.06531E+00
3	6.06531E+00	3.67879E+00
4	3.67879E+00	2.23130E+00
5	2.23130E+00	1.35335E+00
6	1.35335E+00	8.20850E–01
7	8.20850E–01	4.97871E–01
8	4.97871E–01	3.01974E–01
9	3.01974E–01	1.83156E–01
10	1.83156E–01	1.11090E–01
11	1.11090E–01	6.73795E–02
12	6.73795E–02	4.08677E–02
13	4.08677E–02	2.47875E–02
14	2.47875E–02	1.50344E–02
15	1.50344E–02	9.11882E–03
16	9.11882E–03	5.53084E–03
17	5.53084E–03	3.35463E–03
18	3.35463E–03	2.03468E–03
19	2.03468E–03	1.23410E–03
20	1.23410E–03	7.48518E–04
21	7.48518E–04	4.53999E–04
22	4.53999E–04	3.04325E–04
23	3.04325E–04	1.48625E–04
24	1.48625E–04	1.00000E–11

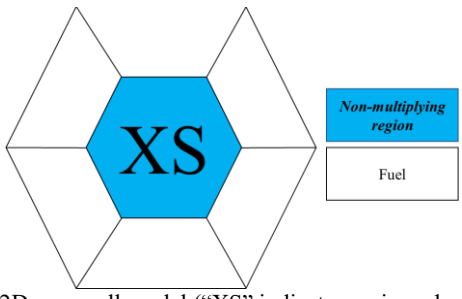

Fig. 3. 2D supercell model ("XS" indicates region where XSs are generated).

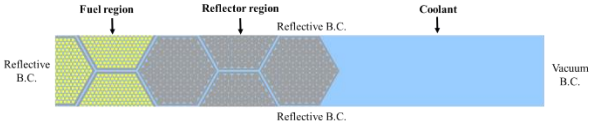

Fig. 4. Radial reflector model.

In this work, the SPH method [5] is applied to correct the flux-volume-weighted XS of the strongly absorbing region and its surroundings, i.e., the control SA and its six-surrounding fuel SAs. The SPH factors are generated using MCS/R2 by a procedure indicated in Fig. 5.

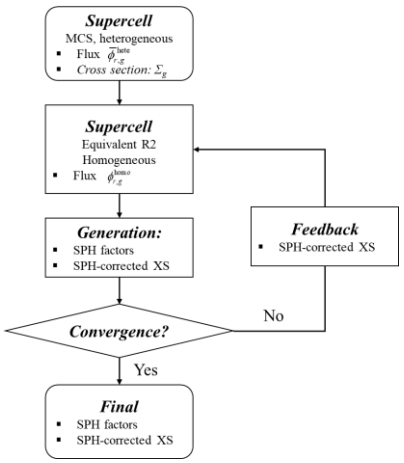

Fig. 5. Iteration scheme for SPH factor generation.

First, a supercell model of the control SA is utilized to generate the heterogeneous transport solution of the fluxes and MG XSs of two regions, i.e., the control SA and its surroundings. The equivalent R2 supercell model is then simulated (Fig. 6) to compute the homogeneous region-wise diffusion fluxes.

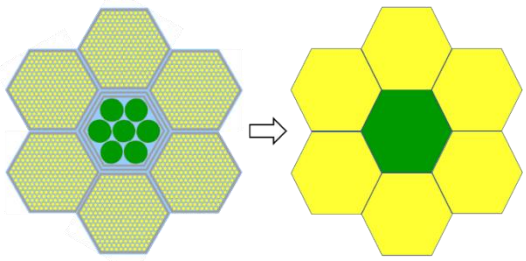

Fig. 6. Heterogeneous MCS (left) and equivalent homogeneous R2 (right) supercell models.

The SPH factors are then generated using an iterative method:

$$SPH_{r,g} = \frac{\bar{\phi}_{r,g}^{\text{hete}}}{\phi_{r,g}^{\text{homo}}} \times Norm_g, \text{ at } i^{th} \text{ iteration} \quad (1)$$

$$Norm_g = \frac{\sum_r V_r \phi_{r,g}^{\text{homo}}}{\sum_r V_r \bar{\phi}_{r,g}^{\text{hete}}} \quad (2)$$

where $\bar{\phi}_{r,g}^{\text{hete}}$ and $\phi_{r,g}^{\text{homo}}$ are the MCS average heterogeneous and R2 homogeneous flux in region r and group g, respectively, and $Norm_g$ is a normalization factor, which is defined in Eq. (2). The modified macroscopic XSs for each region and energy group are then produced using Eq. (3). Note that the fission spectrum remains unchanged during the iteration.

$$\Sigma_{r,g}^{\mathrm{mod}} = SPH_{r,\mathrm{g}} \times \Sigma_{r,g} \quad (3)$$

R2 repeats the simulation until the following conversion criterion is met:

$$\max \frac{\left| SPH_{r,g}^{i} - SPH_{r,g}^{i-1} \right|}{SPH_{r,g}^{i-1}} < 10^{-5} \quad (4)$$

Fig. 7 shows the eigenvalue and SPH factor convergence behavior during the iteration. The eigenvalue rapidly reaches the MCS reference solution after a few iterations and gradually becomes stable. The number of iterations required to make the SPH factor converge is case-dependent, and in the case of MET-1000 core, more than 20 iterations were required to satisfy the convergence criterion of less than 10^{-5}. After being modified by the SPH factors, the control rod XS decreases by factors ranging from 0.58 to 0.90, whereas the fuel XS in the surrounding regions increases by factors of 1.01 to 1.03.

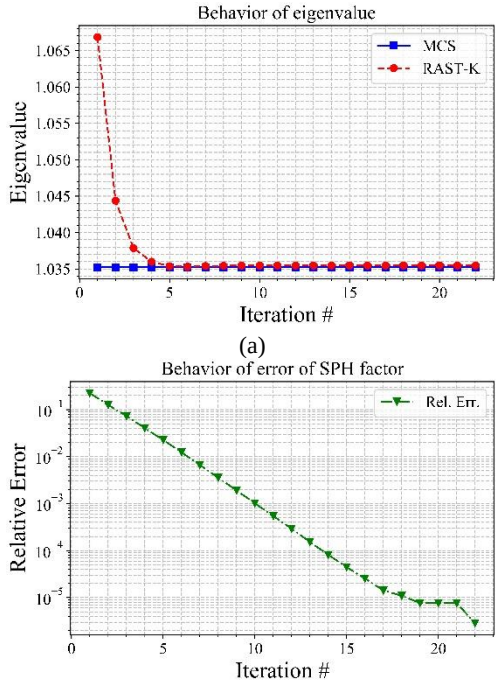

Fig. 7. Convergence of the eigenvalue (a) and SPH factor (b) during iteration.

4.2 Numerical Results

The ENDF/B-VII.0 cross-section library is used for all the simulations, where the temperatures of the fuel and the other materials are set to 900 and 600 K, respectively. The reference solutions are computed using MCS with the criticality set as follows: 5 inactive batches, 20 active batches, 200 cycles per batch, and 20,000 histories per cycle.

The 24-group macroscopic XS data are obtained by MCS and reconstructed into a database that is compatible with the nodal diffusion code R2 to simulate a whole-core problem and predict the core reactivity in the case of un-rodded and rodded state. It is noted that the SPH factor is not used in the un-rodded core problem. In the case of the rodded problem, two approaches are used to apply the SPH factors. In one approach, the XS is modified only in the control SA regions, and in the other, the XS is modified in the control SA region and the surrounding fuel SAs. Fig. 8 shows the power profiles at the un-rodded problem and the root-mean-square (RMS) error in radial and axial power is less than 0.7% and 1.55, respectively.

Table II: Comparison in Core Reactivity

Case	MCS (±4pcm)	MCS/R2 vs. MCS Difference (pcm)		
		no SPH	SPH (only CR)	SPH (CR + fuel)
Un-rodded	1.02995	41	n/a	n/a
Rodded	0.86684	2,681	1,017	-2

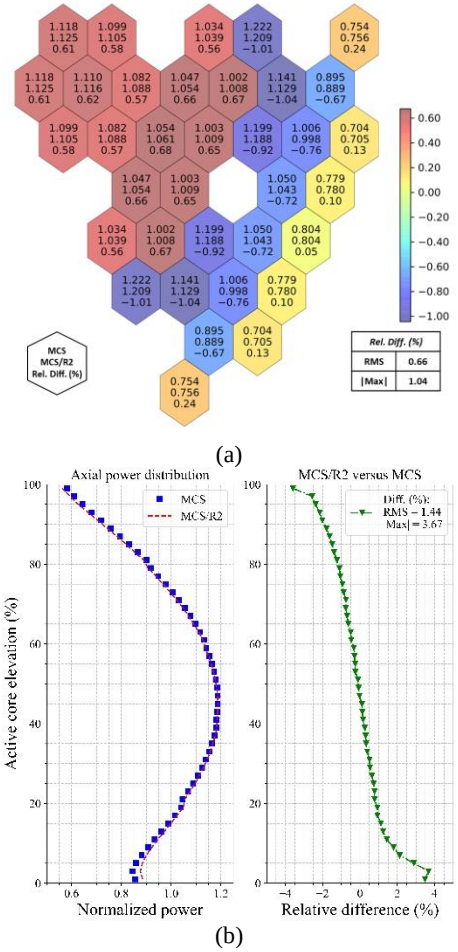

Fig. 8. Radial power distribution (for one-sixth core symmetry, a) and axial power distribution (b) calculated by MCS/R2 and MCS.

The k_{eff} values obtained by 3D whole-core calculation using MCS/R2 and MCS at beginning-of-cycle at the un-rodded and rodded case are summarized in Tables II. For

the un-rodded state, an excellent agreement is seen with the difference in k_{eff} approximately 40 pcm. When no correction is applied in the rodded case, R2 clearly overestimates the effect of the control SAs, by more than 2,600 pcm in reactivity. Better solutions are obtained when the SPH factor is applied only in the control rod region, but the difference in k_{eff} remains large, approximately 1,000 pcm. When the SPH-corrected XSs are used for both the control SA and its surrounding fuel SAs, the R2 solution apparently converges to the MCS one. The error originates mainly from the control rod XS, and further improvement is obtained when introducing the correction to its surrounding regions. Therefore, this analysis suggests that the SPH factor should be applied to both the control SAs and their surrounding fuel SAs. When the SPH factor is applied, not only the reactivity but also the radial power distribution is predicted more accurately. Fig. 9 presents the radial power distributions without and with the SPH factors. An overall decrease in the RMS and maximum power error is clearly observed. It is noted that the SPH factor negligibly affects to the axial power distribution. Overall, SPH correction is thus essential for highly accurate analyses of fast reactors.

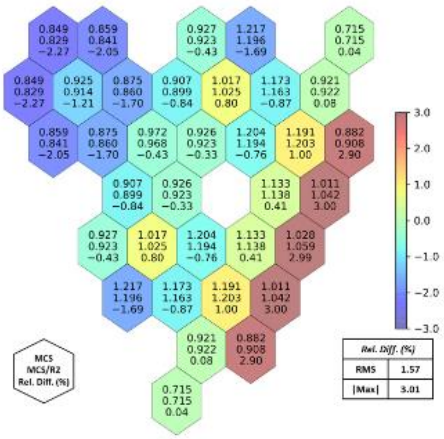

(a)

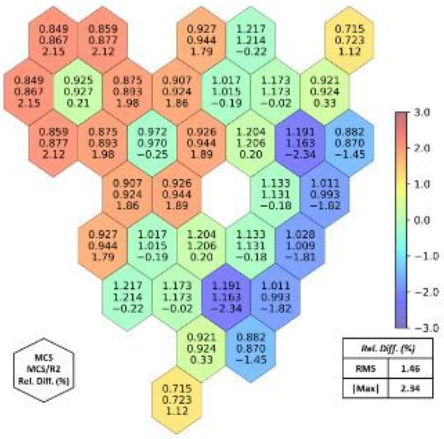

(b)

Fig. 9. Radial power distribution (for one-sixth core symmetry) without SPH factors (a) and with SPH factors (b) calculated by MCS/R2 and MCS.

5. Conclusions

The feasibility of using the SPH method to the code sequence MCS/R2 was investigated, in which the SPH factor aims to correct XSs in the strong absorber region and its surroundings. A code-to-code comparison between the MC code MCS and MCS/R2 was conducted with the un-rodded and rodded 3D whole-core problems to evaluate the potential of the SPH method. Overall, the great prediction of the rodded core reactivity as applying SPH factors was achieved by reducing the reactivity difference by more than 2,600 pcm. Further improvement in radial power distribution was obtained as decreasing the RMS and maximum difference comparing to the MCS reference solutions. Therefore, it is successfully demonstrated that the SPH method is a valuable access for fast reactor analysis.

ACKNOWLEDGEMENT

This work was supported by the National Research Foundation of Korea (NRF) grant funded by the Korea government (MSIT). (No.NRF-2017M2A8A2018595)

REFERENCES

[1] N.E. Stauff, T.K. Kim, T.A. Taiwo, et al., *Benchmark for Neutronic Analysis of Sodium-cooled Fast Reactor Cores with Various Fuel Types and Core Sizes* (No. NEA-NSC-R--2015-9), Organization for Economic Co-Operation and Development, 2016.

[2] H. Lee, W. Kim, P. Zhang, M. Lemaire, A. Khassenov, J. Yu, Y. Jo, J. Park, D. Lee, MCS–A Monte Carlo particle transport code for large-scale power reactor analysis, *Ann. Nucl. Energy 139* (2020) 107276.

[3] T.D.C. Nguyen, T.Q. Tran, H. Lee, D. Lee, Group Constants Generation using MCS Monte Carlo Code for Fast Reactor Analysis, in: *Proceedings of the Korean Nuclear Society Autumn Meeting, Changwon, Korean, December 16–19, 2020.*

[4] T.Q. Tran, A. Cherezov, X. Du, J. Park, D. Lee, Development of hexagonal-Z geometry capability in RAST-K for fast reactor analysis, in: *19th International Conference on Emerging Nuclear Energy Systems (ICENES 2019), Bali, Indonesia, October 6–9, 2019.*

[5] E. Nikitin, E. Fridman, K. Mikityuk, On the use of the SPH method in nodal diffusion analyses of SFR cores, *Ann. Nucl. Energy 85* (2015) 544–551.